Effective properties of evolving porous media: From microstructure to macroscopic scale

Maria OLARTE-GARZON, Jean-Michel PEREIRA, Patrick DANGLA

A variety of “frozen” geomaterials

Complex behavior, complex microstructure, high heterogeneity

Example: Batagaika megaslump

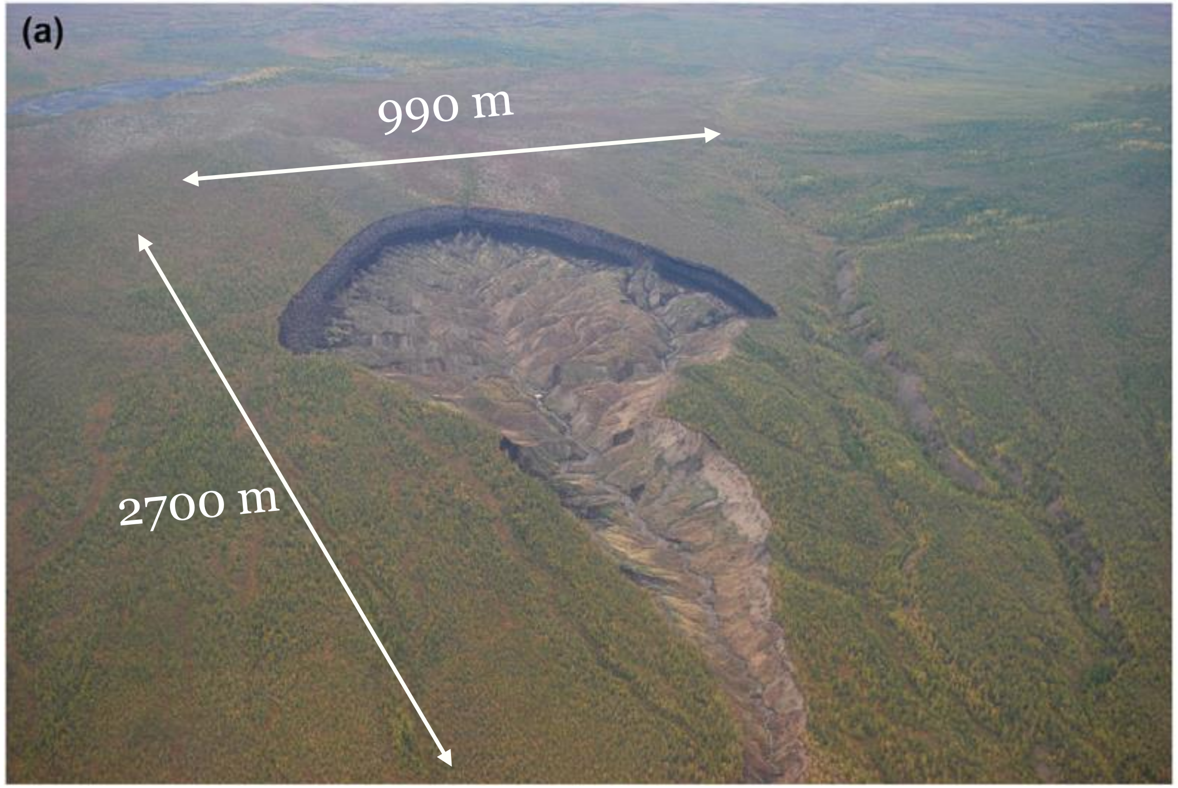

Frozen soils and permafrost in cold regions (ground at or below 0°C for >= 2 consecutive years) provides a key role for foundation stability for infrastructure (roads, pipelines, buildings).

Murton, J., Opel, T., Wetterich, S., Ashastina, K., Savvinov, G., Danilov, P., & Boeskorov, V. (2023). Batagay megaslump: A review of the permafrost deposits, Quaternary environmental history, and recent development. Permafrost and Periglacial Processes, 34(3), 399-416.

What is periodic homogenization?

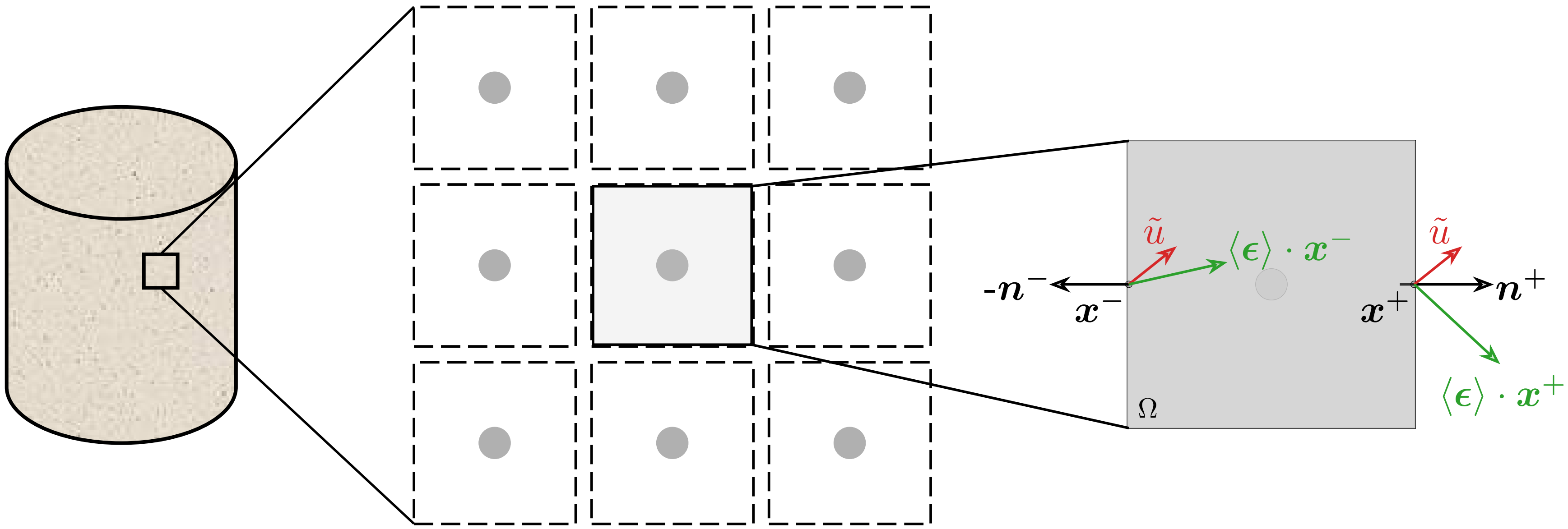

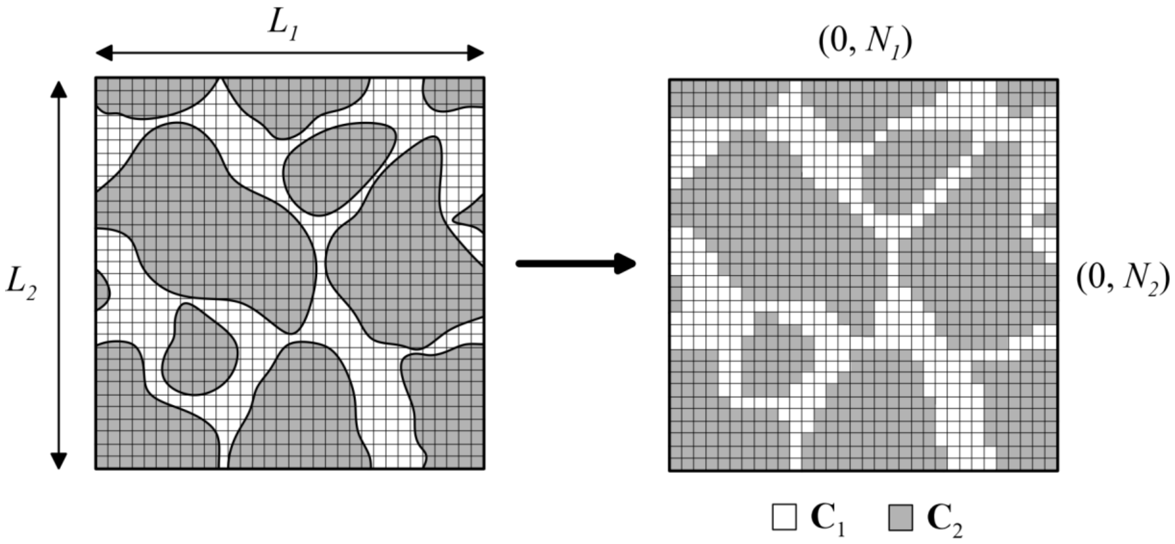

FFT-based homogenisation:

Resolution of a Lippman-Schwinger equation (Moulinec & Suquet, 1994)

Issues with infinite contrasts, treated following Sab et al. (2024)

Thermoporomechanical couplings

Constitutive relations of the porous solid (Coussy, 2011):

Mechanical

$$\underline{\underline{\Sigma}} = \mathbb{C}^{hom} : \underline{\underline{E}} - \underline{\underline{B}}^{hom} P - \mathbb{C}^{hom} : \underline{\underline{A}}^{hom} T$$

Hydraulic

$$\Phi - \phi_0 = \underline{\underline{B}}^{hom} : \underline{\underline{E}} + \frac{1}{N^{hom}} P - 3A_{\phi}^{hom} T$$

$$\underline{W} = -\frac{\rho}{\eta} \underline{\underline{K}}^{hom} \cdot \underline{\nabla P}$$

Thermal

$$S_s = \mathbb{C}^{hom} : \underline{\underline{A}}^{hom} : \underline{\underline{E}} - 3A_{\phi}^{hom} P + H^{hom} T$$

$$\underline{Q} = -\underline{\underline{\Lambda}}^{hom} \cdot \underline{\nabla T}$$

Mechanical | Hydraulic | Thermal

$\underline{\underline{E}}$: Macroscopic strain

P: Macroscopic pore pressure

T: Macroscopic temperature

$\underline{\underline{\Sigma}}$: Macroscopic stress

Φ: Macroscopic porosity

S_s: Macroscopic solid skeleton's entropy

$\underline{W}$: Macroscopic flux vector

$\underline{Q}$: Macroscopic heat vector

Coussy (2011). Mechanics and physics of porous solids. John Wiley & Sons.

Numerical tool

JANUS library[1]

Discretization of Lippmann-Schwinger equation

Extension of the library to:
- Thermohydraulics

Newton-Raphson

Complex transformations

Visualization

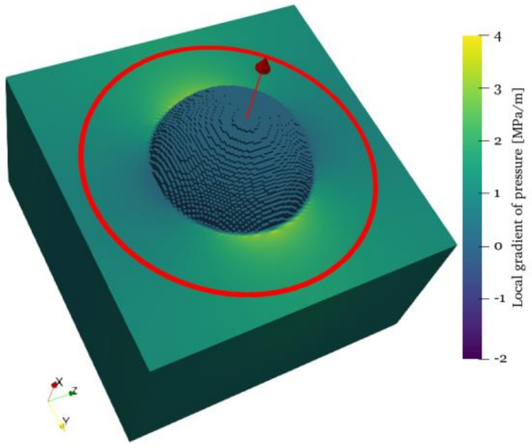

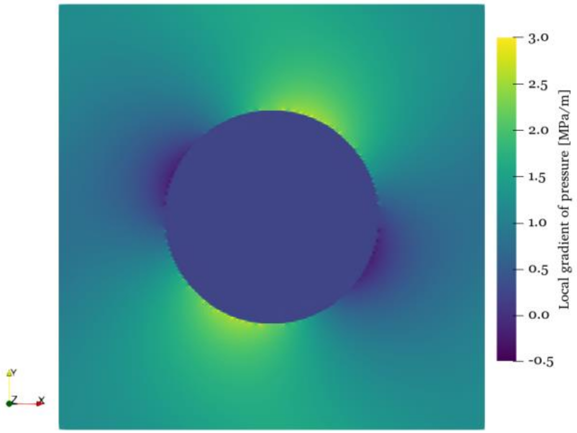

[1] Sébastien Brisard

Application:
Nucleation and sublimation in lunar soils

LUNAR REGOLITH SIMULANT

Real image

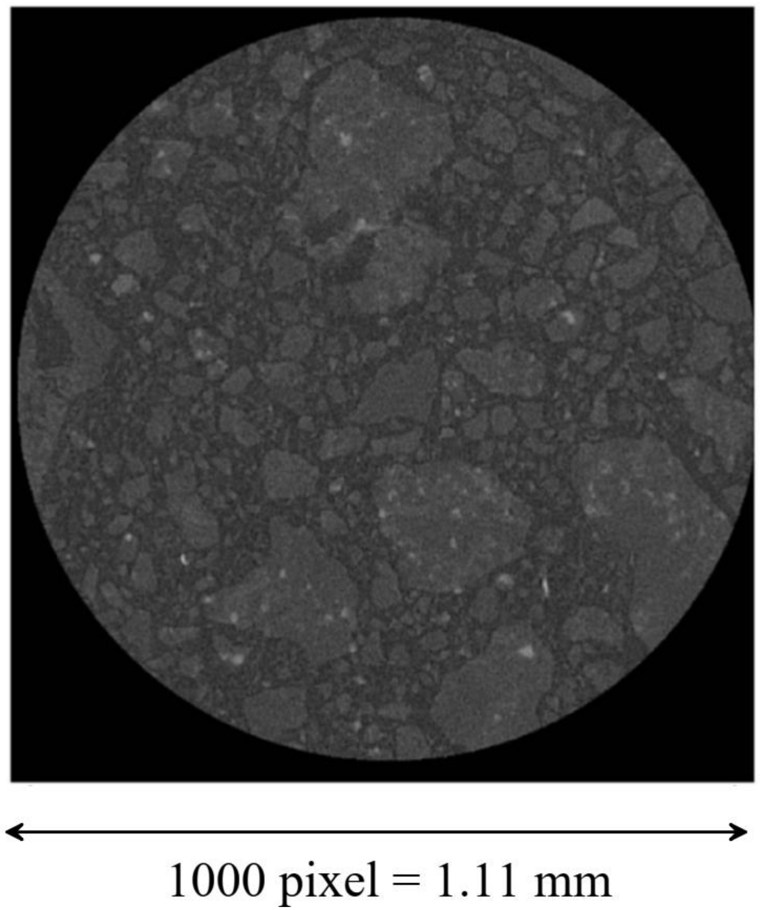

Discretized image

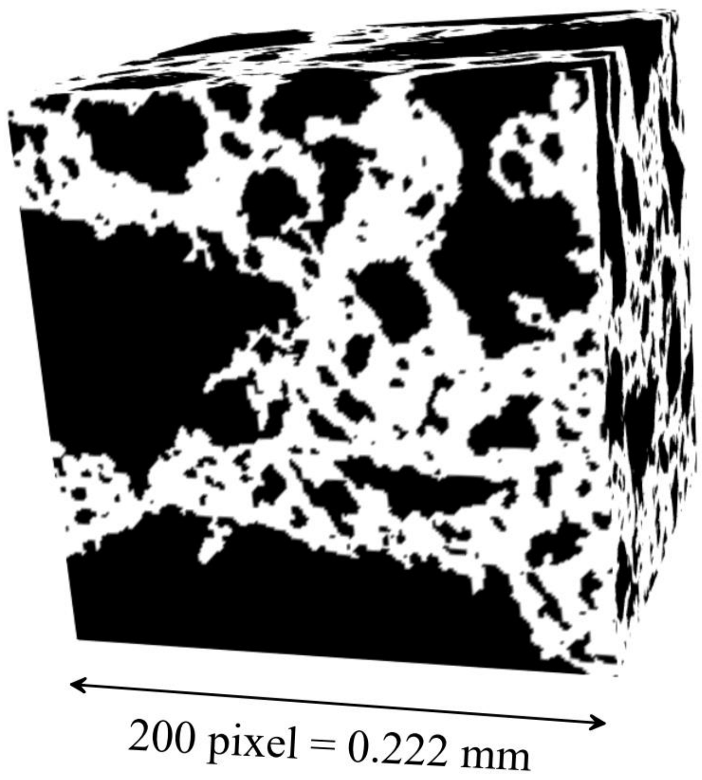

Simulant properties:

The simulant consists of plagioclase, pyroxene, ilmenite, and glass.

Pixel size of 1.11 μm

The complete digital consists of 1000 × 1000 × 1000 voxels.

Kunimasu, T., Sawayama, K., & Tsuji, T. (2023). Estimation of the mass fraction and distribution of ice in a lunar regolith simulant from seismic velocity. Icarus, 406, 115725.

Soil Freezing Characteristic Curve (SFCC)

Pore-morphology-based estimation

Binary image

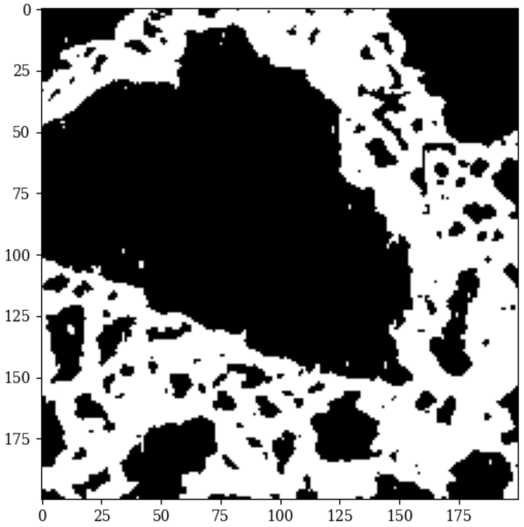

Distance map

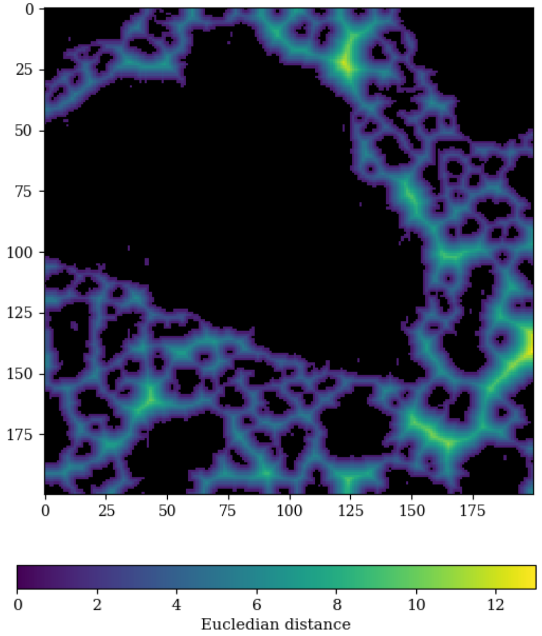

Eroded image

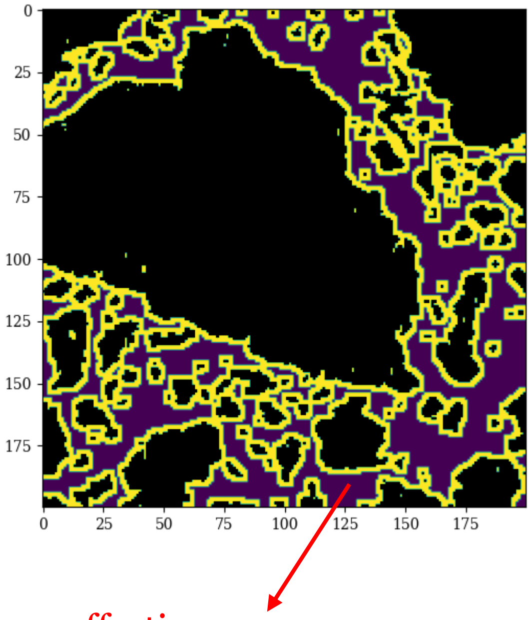

Openend image

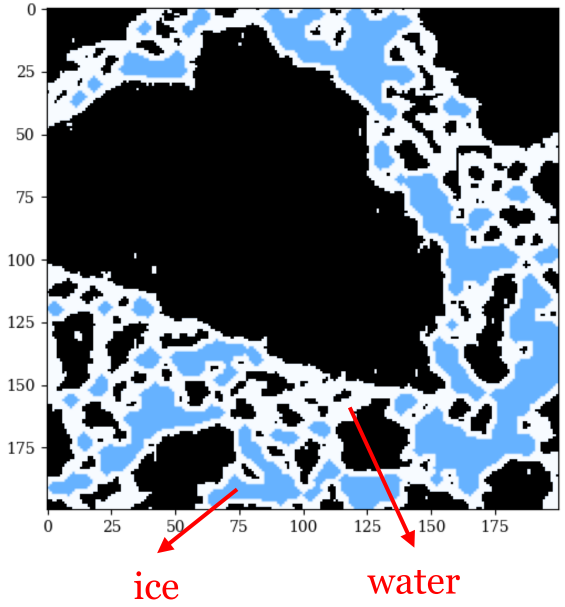

$$d(\hat{\boldsymbol{x}}_p) = \min_{\hat{\boldsymbol{x}}_s \in X_s} ||\hat{\boldsymbol{x}}_p - \hat{\boldsymbol{x}}_s||_2$$

$$X_p^{eff} = \{\hat{\boldsymbol{x}}_p | d(\hat{\boldsymbol{x}}_p) \geq \hat{r}_p(T)\}$$

Gibbs-Thompson equation:

$$\hat{r}_p(T) = \frac{3\sigma_{iw}\cos\theta}{\rho_i L_f}\left(1 - \frac{T}{T_f^{\infty}}\right)^{-1}$$

Suh, H. S., Na, S., & Choo, J. (2024). Pore-morphology-based estimation of the freezing characteristic curve of water-saturated porous media. Water Resources Research, 60(8), e2024WR037035.

Soil Freezing Characteristic Curve (SFCC)

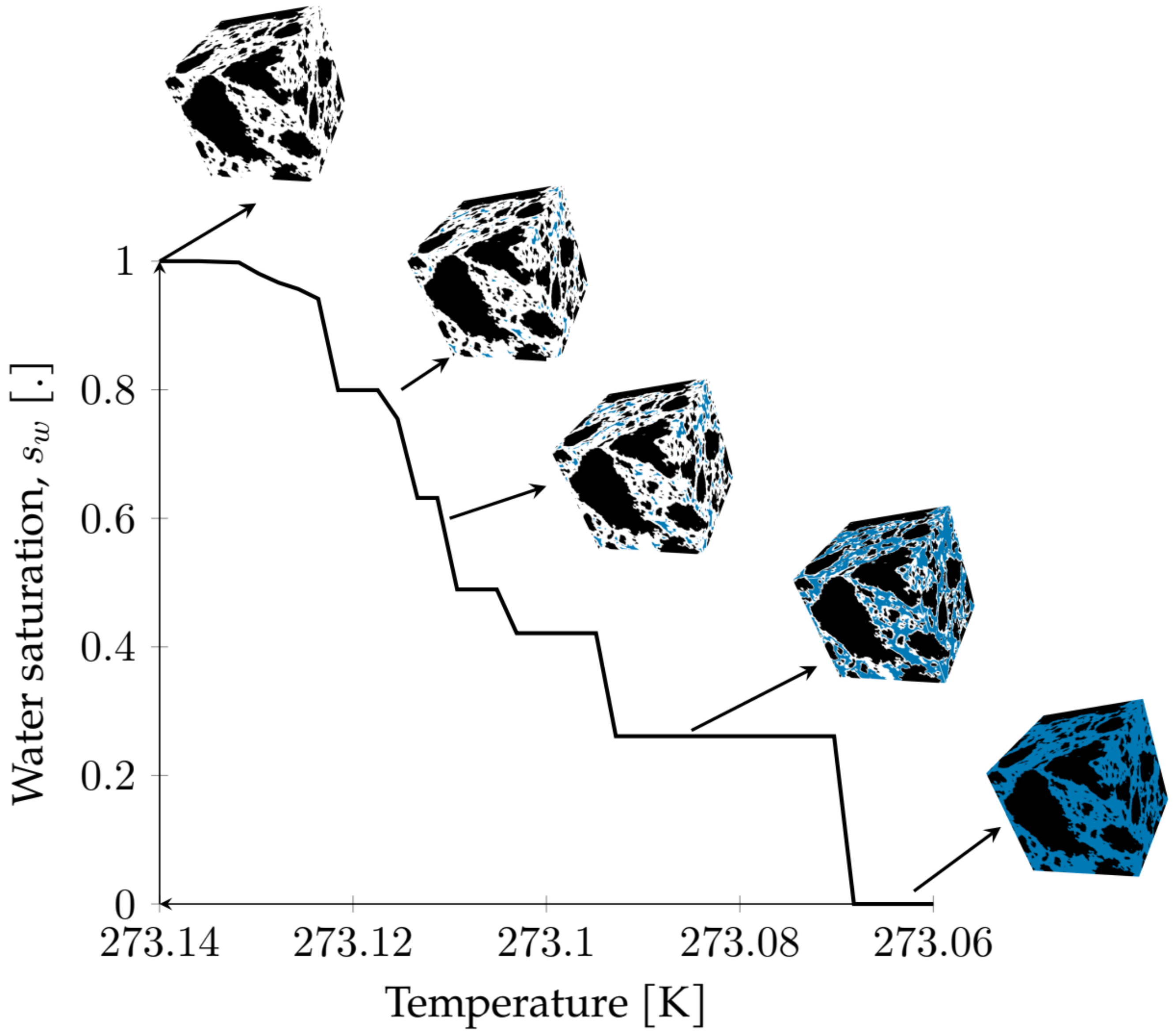

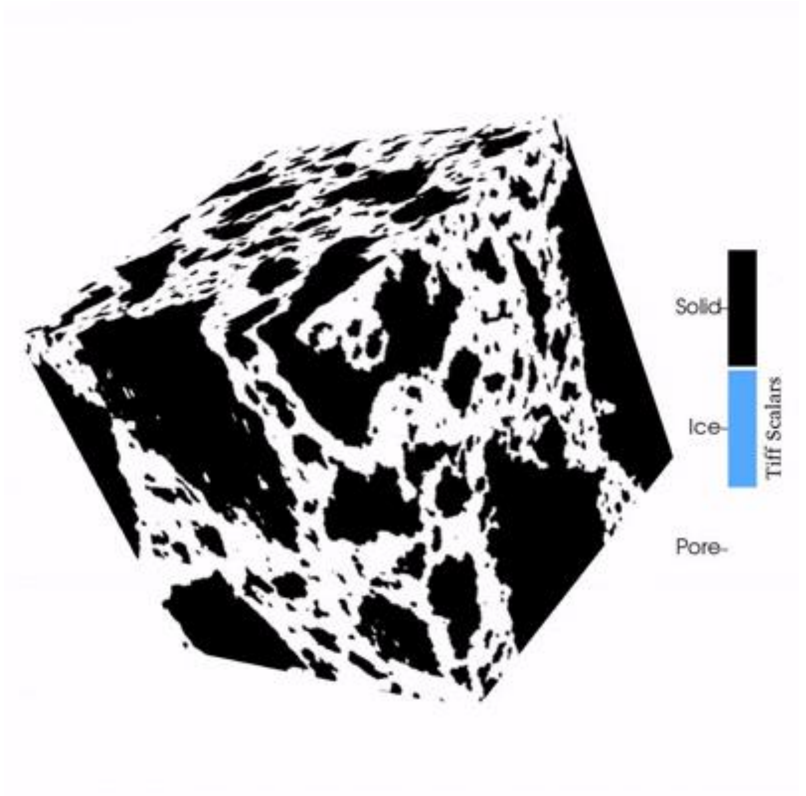

Temperature variaties from 273.14 K to 273.06 K, and s_w was recorded at 40 intervals of 0.002 K.

The ice density was kept constant at ρ_c = 910 kg/m³.

ELASTICITY

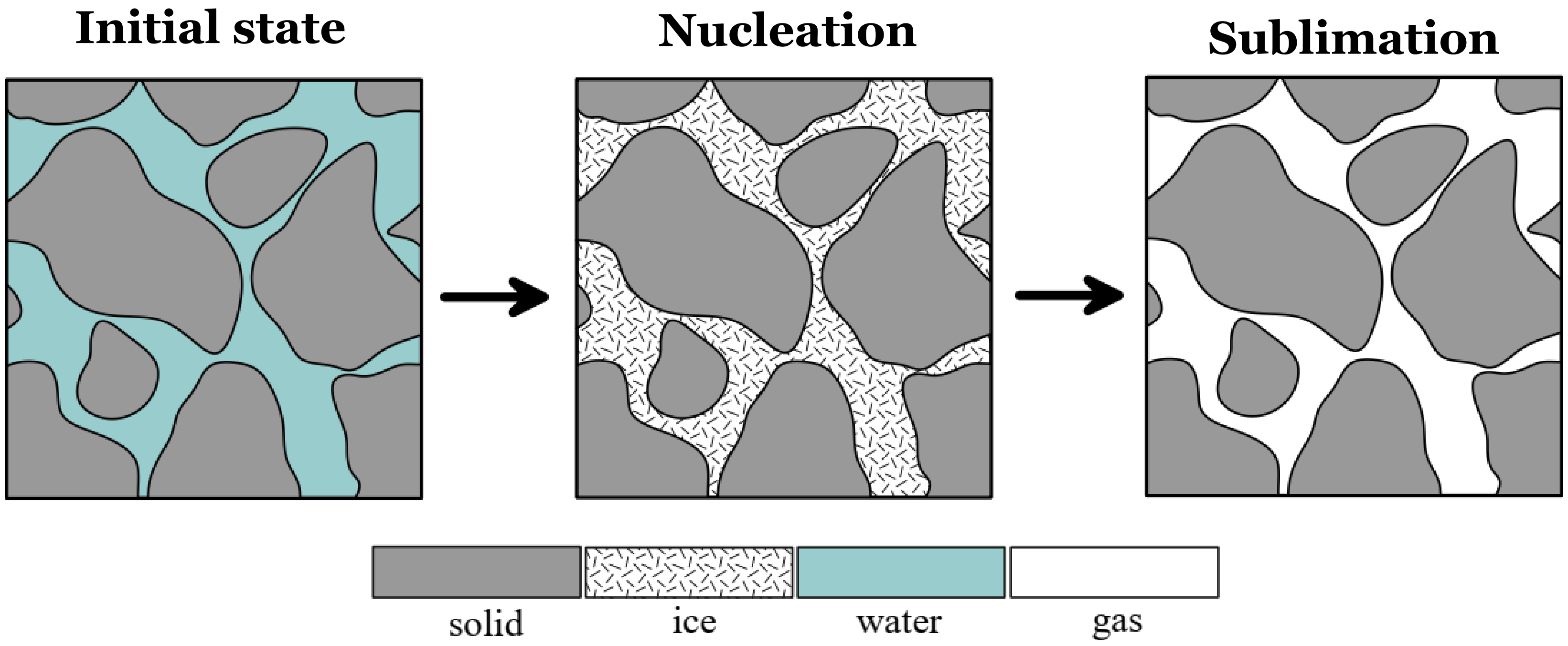

Input parameters of the phases for the FFT-based simulations.

	Mechanics			Transport			
Phase	k [GPa]	g [GPa]	ν [-]	d_{CO2} [m^2/s]	λ [W/(m·K)]	μ [Pa · s]	ν [-]
Solid	7.97	4.89	0.24	0.0	0.001* [123], 0.1 [121]	∞	0.5
Water	2.2	0.0	0.5	$1.6 \cdot 10^{-9}$ [124]	0.6 [125]	$1 \cdot 10^{-3}$	0.5
Ice	9.2	3.3	0.33	0.0	2.2 [125]	∞	0.5
Gas	0.0	0.0	0.0	$1.6 \cdot 10^{-5}$ [107]	0.0	-	-

Note: * corresponds to the value under lunar vacuum conditions.

Loading cases and boundary conditions

Shearing

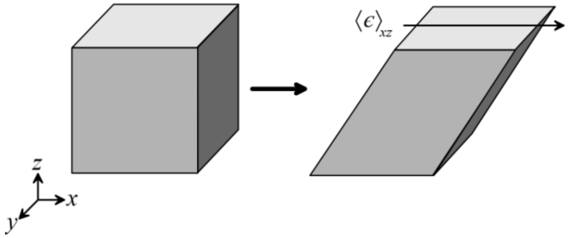

$$d\langle\boldsymbol{\sigma}\rangle_{xz} = G \times 2\, d\langle\boldsymbol{\epsilon}\rangle_{xz}$$

Isotropic

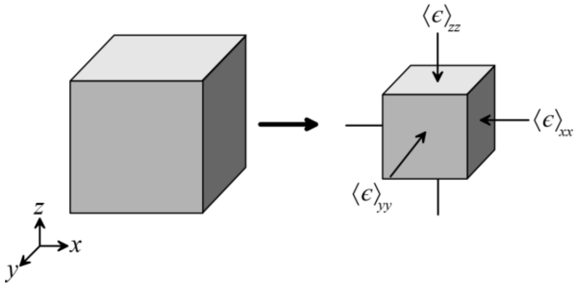

$$d\langle\boldsymbol{\sigma}\rangle_{v} = K \times d\langle\boldsymbol{\epsilon}\rangle_{v}$$

Oedometric

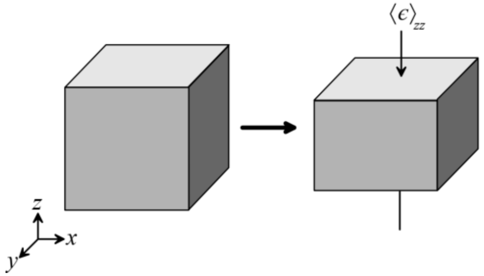

$$d\langle\boldsymbol{\sigma}\rangle_{zz} = E_{oedo} \times d\langle\boldsymbol{\epsilon}\rangle_{zz}$$

$$\nu = \frac{k_0}{1+k_0} = \frac{d\,P_{lat}}{d\,P_{load} + d\,P_{lat}}$$

$$E = E_{oedo}\frac{(1+\nu)(1-2\nu)}{1-\nu}$$

Transport

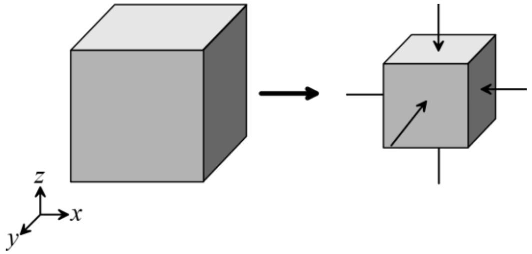

$$\langle \boldsymbol{q} \rangle = -\boldsymbol{\lambda}^{hom} \cdot \langle \boldsymbol{\nabla}(\theta) \rangle$$

$$\langle \boldsymbol{w} \rangle = -\frac{\rho}{\eta}\boldsymbol{k}^{hom} \cdot \langle \boldsymbol{\nabla}(p) \rangle$$

$$\langle \boldsymbol{j} \rangle = -\boldsymbol{d}^{hom} \cdot \langle \boldsymbol{\nabla}(c) \rangle$$

Elastic moduli as a function of water saturation

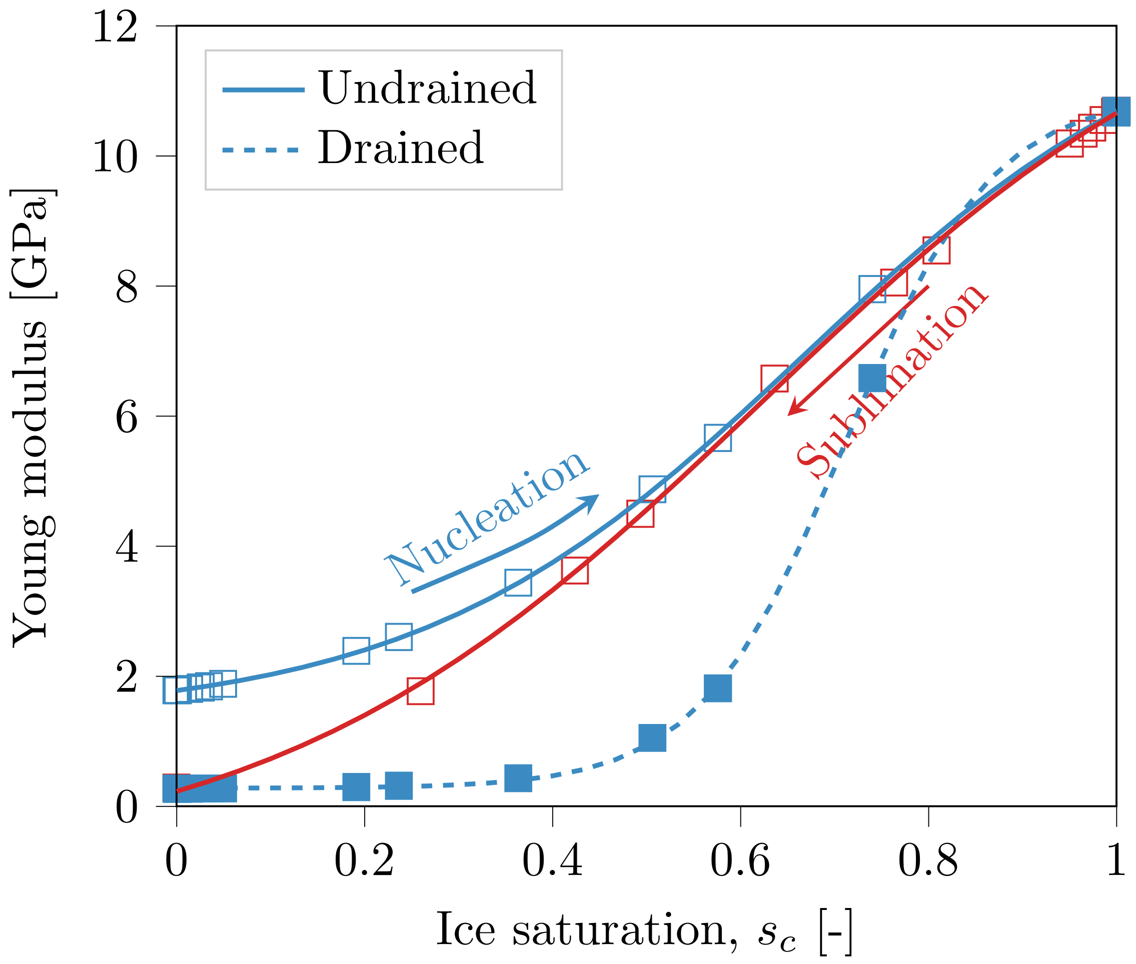

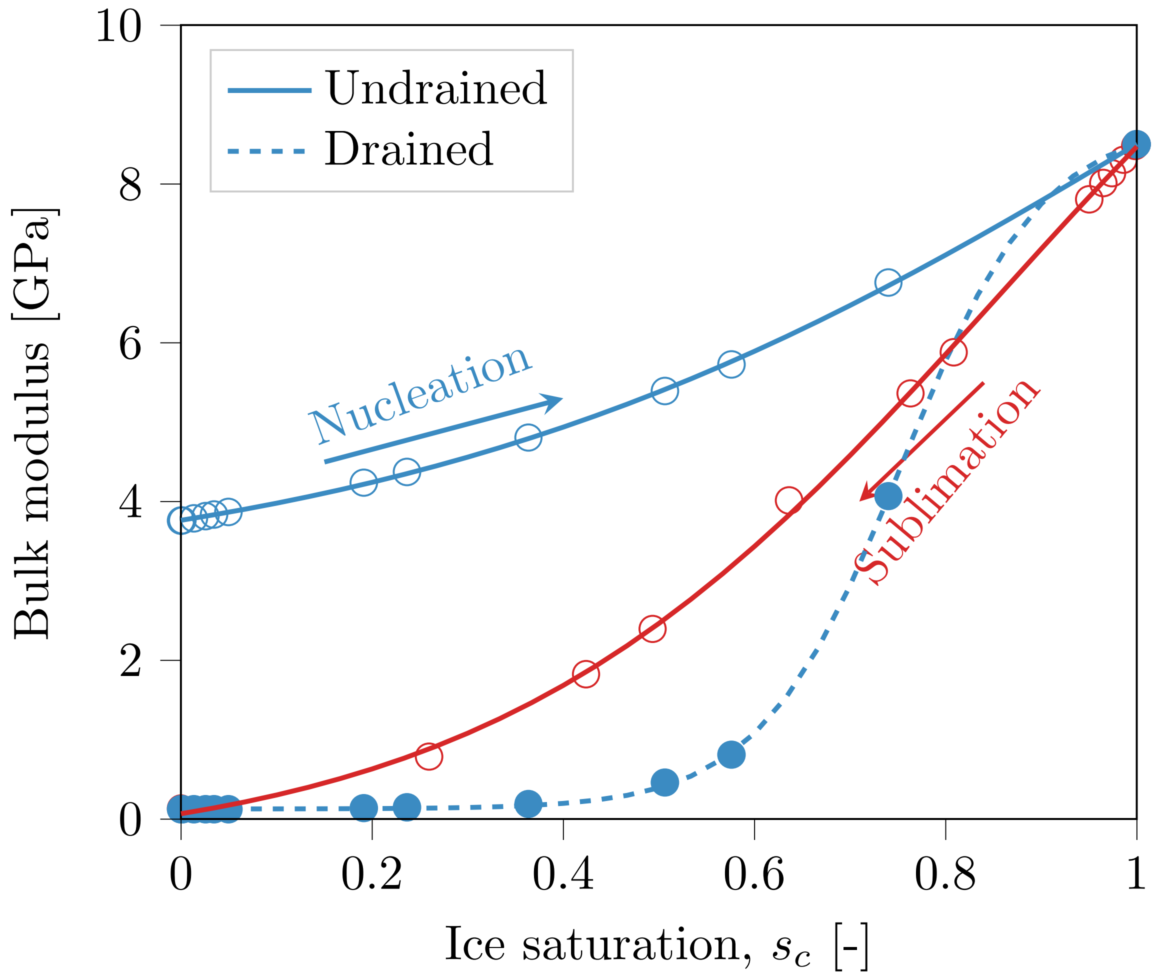

Elastic moduli as a function of water saturation

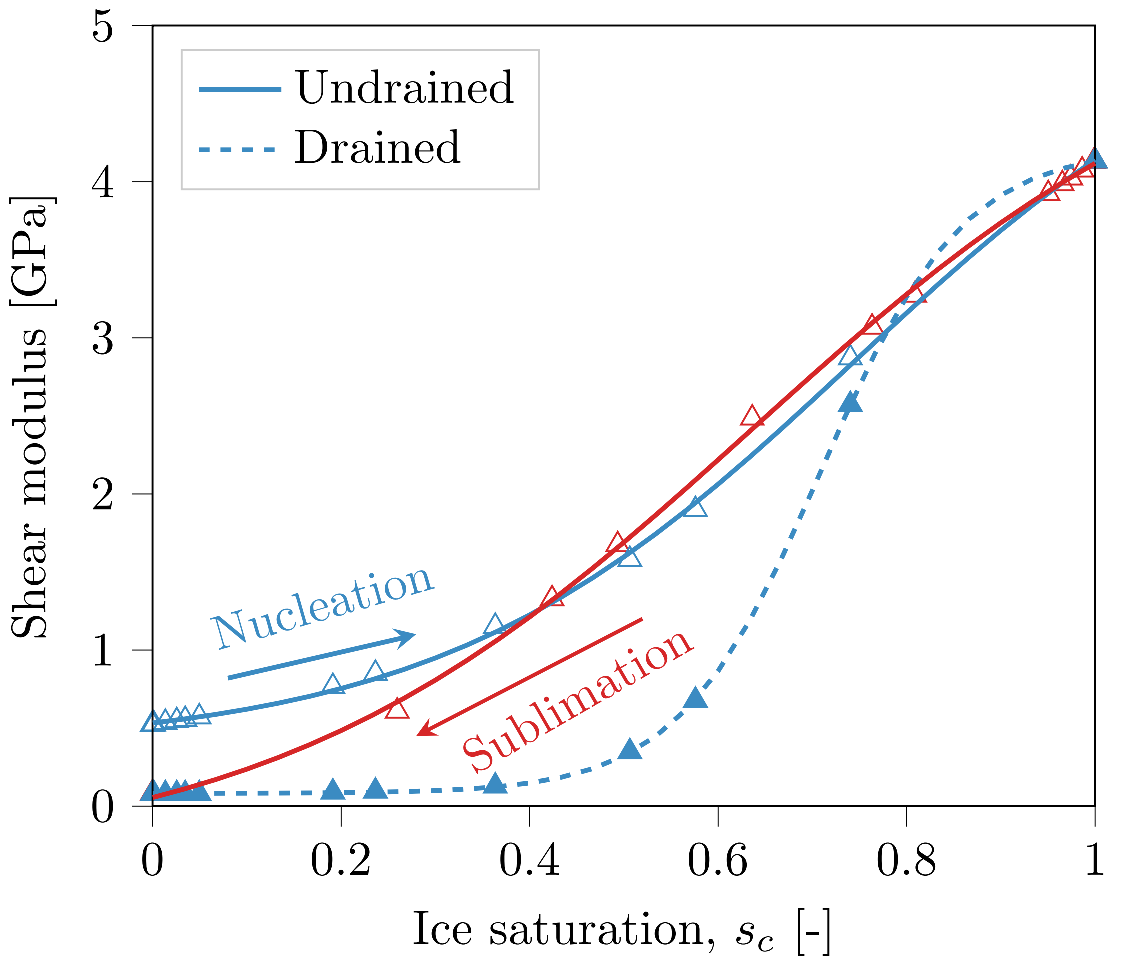

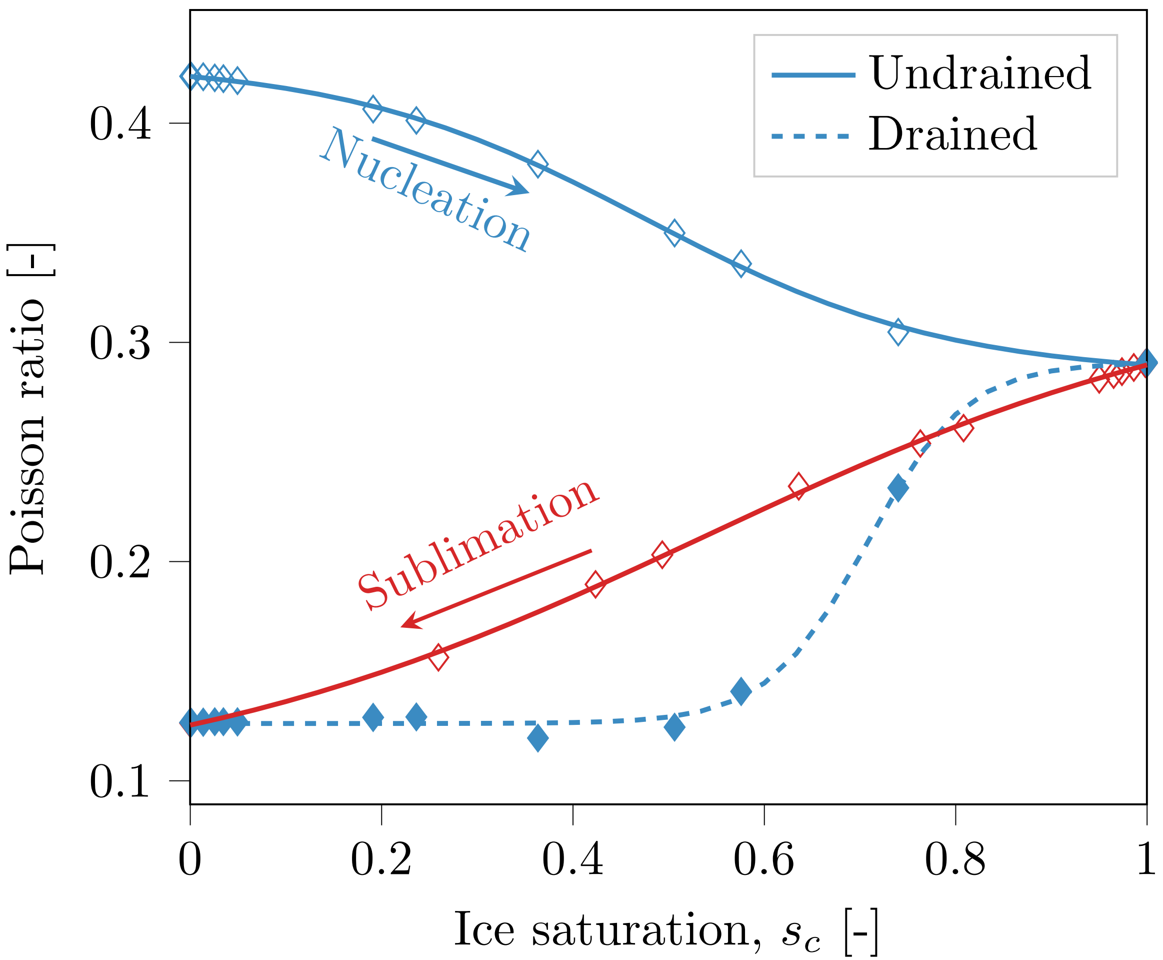

Transport properties during ice nucleation

Nucleation

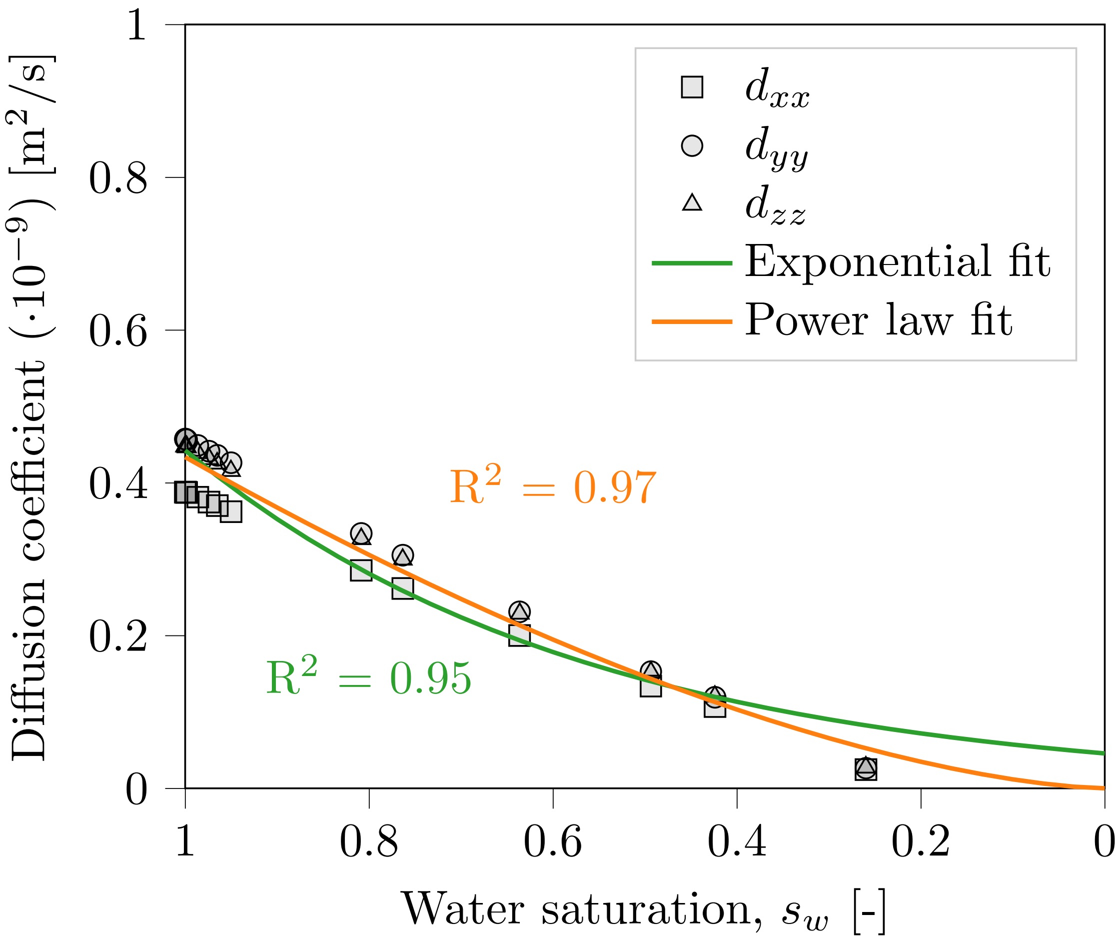

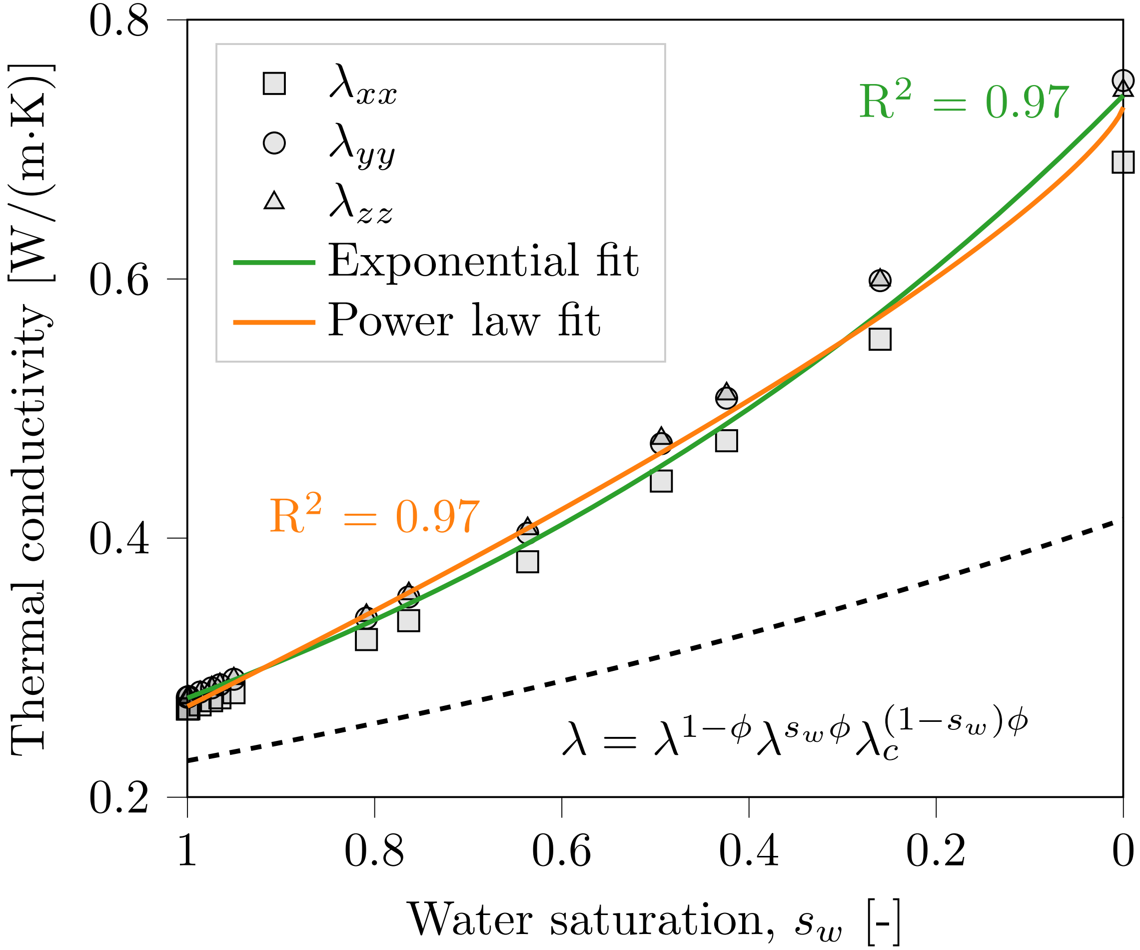

Nucleation

Summary of the permeability models used as comparison.

Model	Equation	Abbreviation	Reference
Brooks-Corey	$k(s_w) = k_{sat} s_w^{\frac{2+3\lambda}{\lambda}}$	B-C	[128]
van Genuchten-Mualem	$k(s_w) = k_{sat}\sqrt{s_w}\left[1-\left(1-s_w^{1/n}\right)^n\right]^2$	vG-M	[129, 130]
Corey type	$k(s_w) = k_{sat} s_w^n$	Corey	[131]

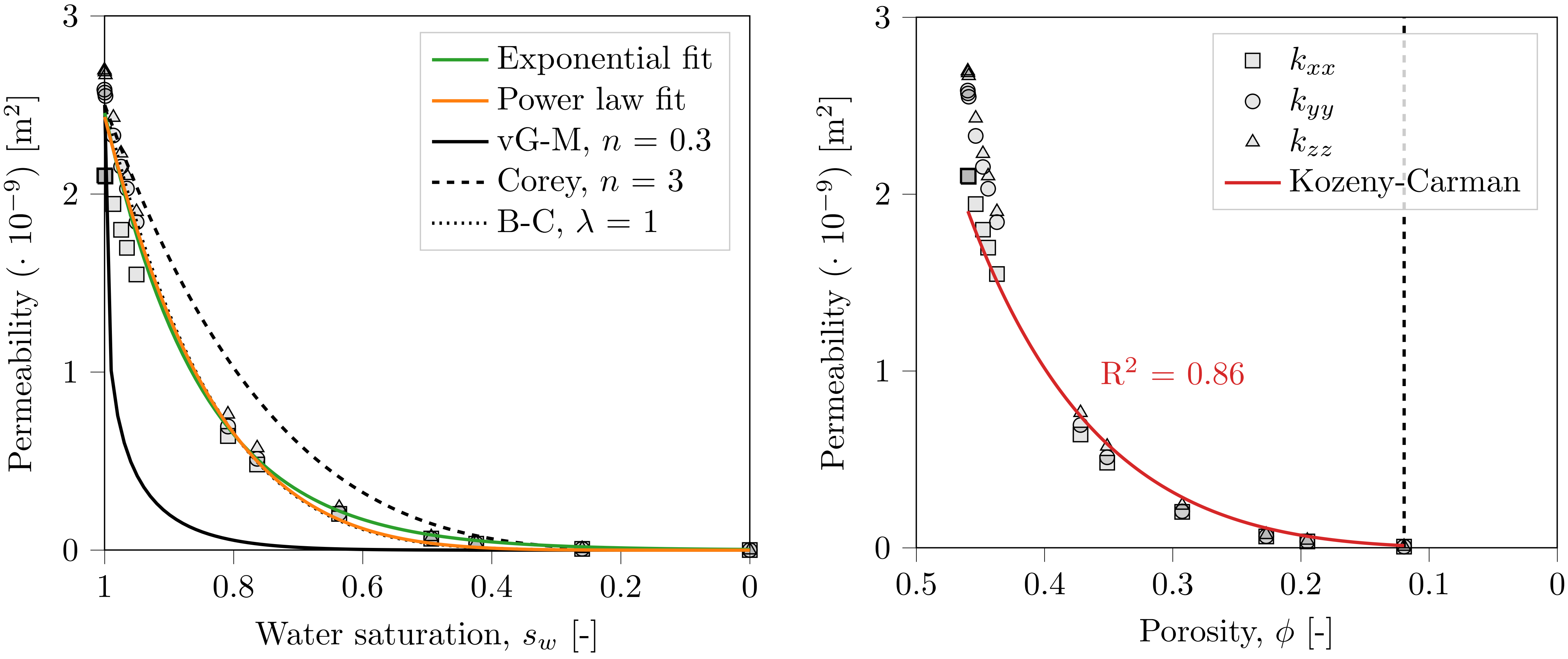

Relationship between seismic velocities and the mass fraction of ice

Sublimation

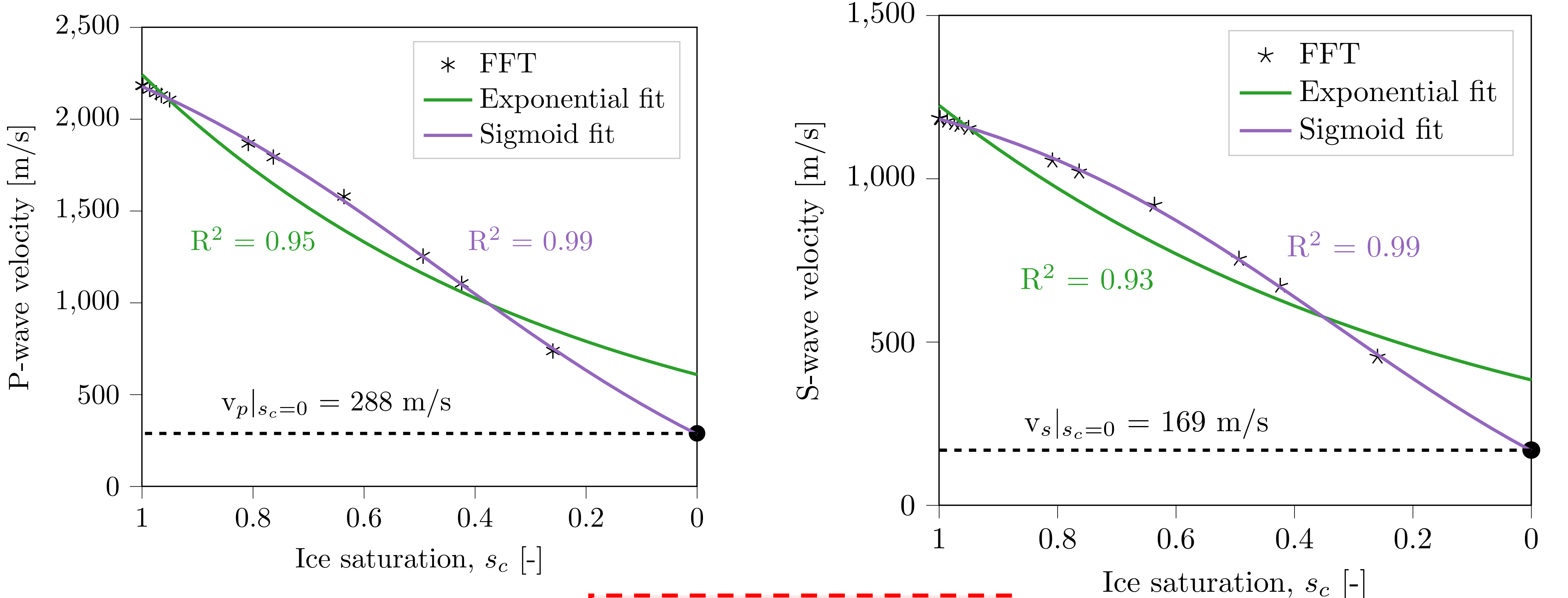

Experimental results:

v_p = 170 m/s, v_s = 110 m/s

PLASTICITY

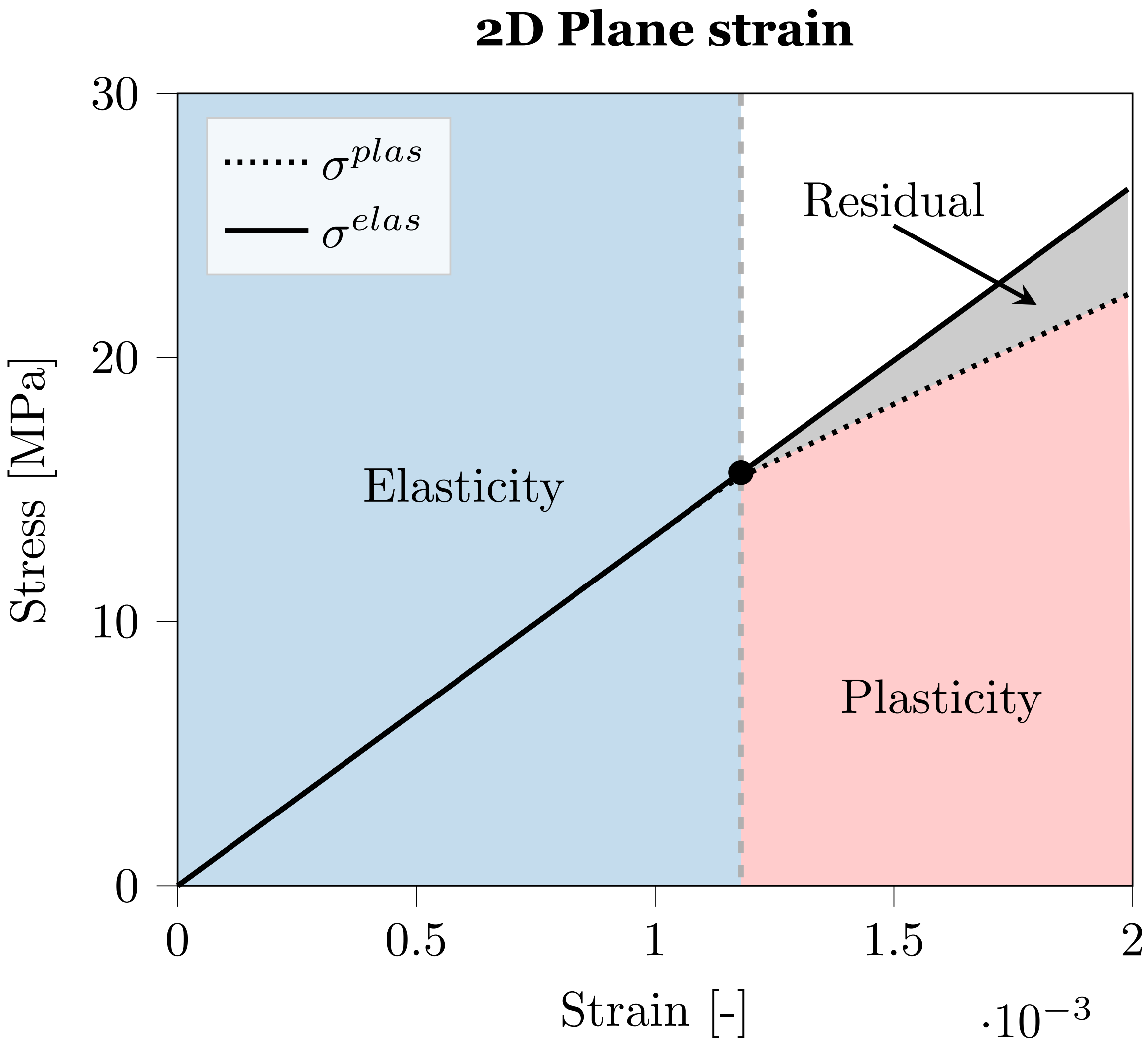

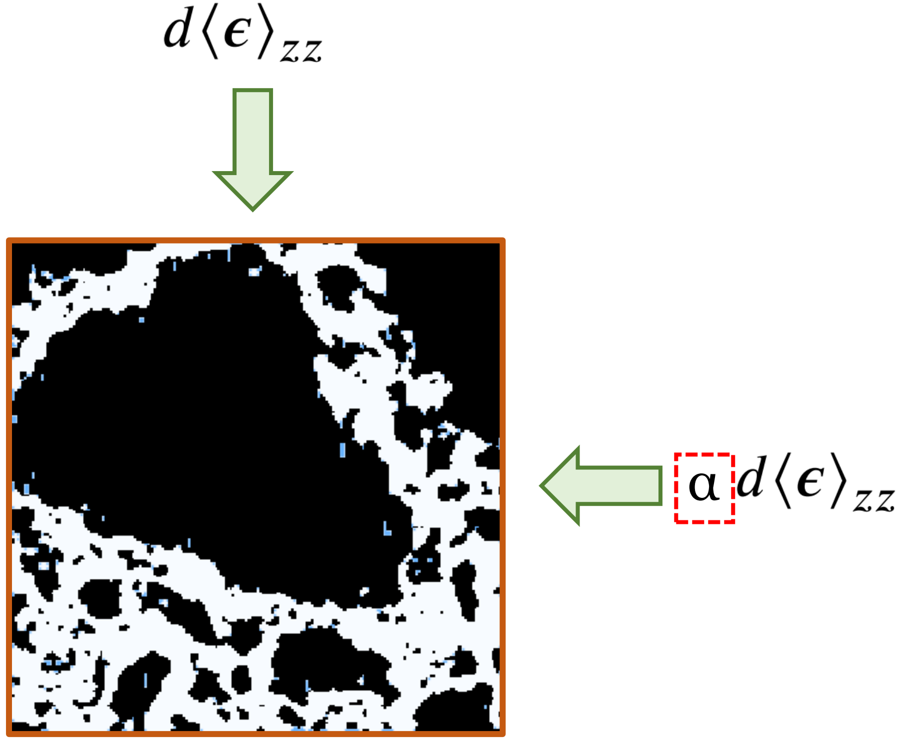

	E [GPa]	ν [.]	yield strength (von Mises' criterion) [MPa]
Regolith	7.97	0.24	-
Water	2.2	0.48	-
Ice	9.2	0.33	13.34

Parameters of the three-phase microstructure used for the elastoplastic homogenization in frozen lunar soils.

Yield surface as a function of ice content

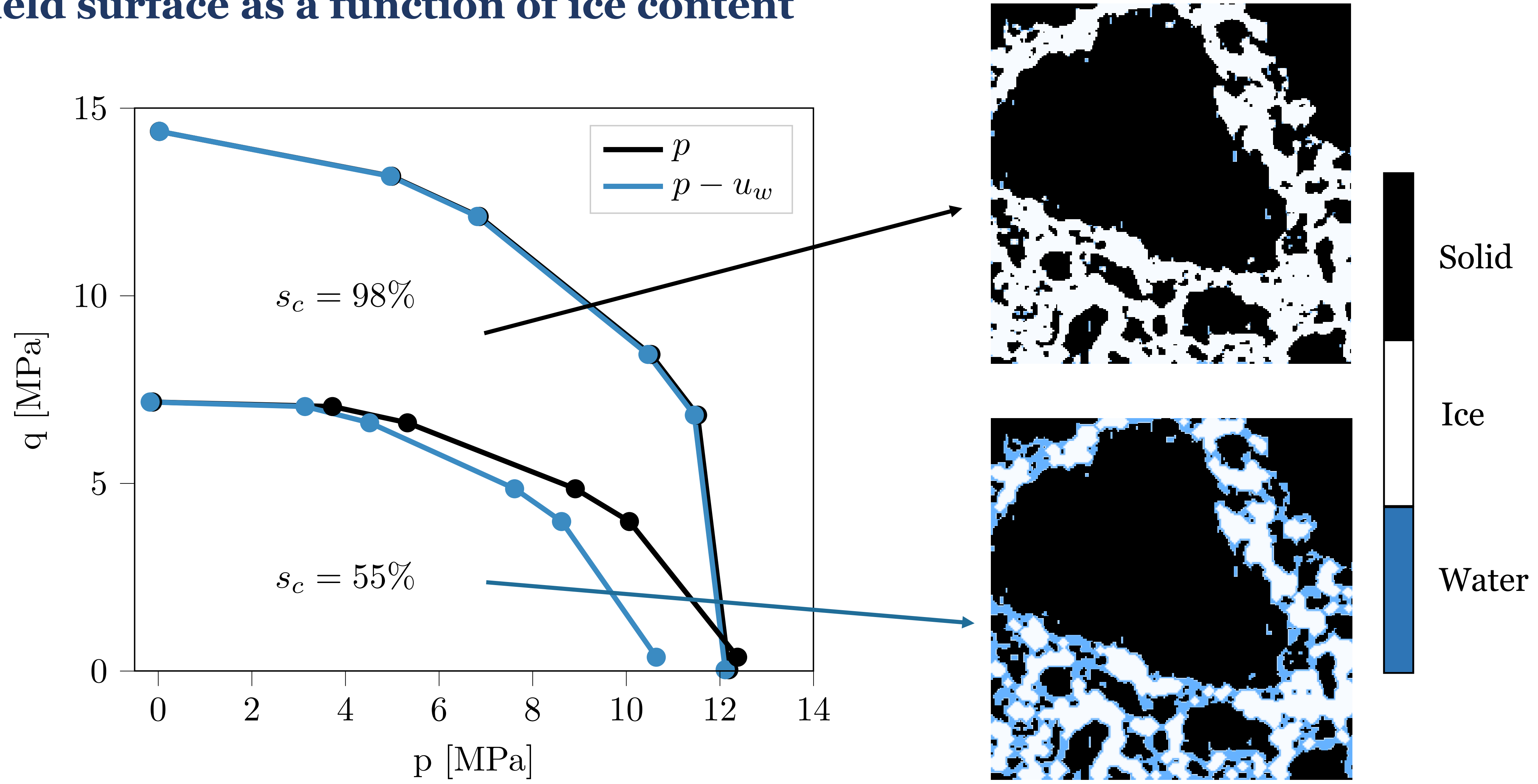

Conclusions

1. The proposed FFT-based approach accounts for thermo-hydro-elastoplastic behavior, enabling the computation of the **homogenized operators of the full THM constitutive matrix**.

2. The method remains well-defined even in the limiting cases **of infinitely soft or infinitely stiff materials**.

3. The framework is implemented and validated **for two- and three-dimensional** representative volume elements, ensuring applicability to a wide range of microstructural analyses.

Thank you